



Study of the Effect of Sensor Location on Sonic Echo/Impulse Response Testing in Timber Piles

S. Rashidyan^{1,*}, T.-T. Ng², A. Maji²

¹ Department of Engineering Technology, University of North Texas, Texas, USA.

² University of New Mexico, New Mexico, USA.

ABSTRACT: Nondestructive Testing (NDT) methods have been utilized to assess the conditions of civil infrastructure in the past decades. Among various NDT methods, Sonic Echo / Impulse Response (SE/IR) is a versatile method to characterize unknown bridge foundations. Numerous numerical and experimental studies have been performed regarding the effect of influencing factors such as the pile-to-soil stiffness ratio, length-to-diameter ratio of the pile, presence of defects and anomalies near the pile head, striking method, and hammer type on the success of the SE/IR method. However, there is a lack of comprehensive study regarding the effect of the sensor location on the SE/IR testing results in timber piles. In the current study, challenges about the location of the sensor are investigated by conducting SE tests on bridges with known and unknown foundations. The results obtained from two accelerometers mounted on the side of the piles showed that the measured length of the piles was more consistent from the accelerometer mounted closer to the top of the pile. The success rate of the SE tests from the top accelerometer was 21.6% greater than the bottom accelerometer. The results of this study were confirmed by numerical simulations. Finally, the Impulse Response (IR) analysis was conducted to support the results. The conducted IR analysis showed that the success rate for the top accelerometer was greater than the bottom accelerometer.

Review History:

Received: Jun. 12, 2019
Revised: Apr. 07, 2020
Accepted: Dec. 10, 2019
Available Online: Apr. 07, 2020

Keywords:

Sonic Echo
Impulse Response
Foundation
Pile
Bridge

1- Introduction

For approximately 10 percent of the estimated 600,000 bridges that span waterways in the United States, the “as-built” information - that is, the details of the final structure - is not available or is missing [1]. The National Bridge Inventory (NBI) of the Federal Highway Administration (FHWA) classifies these as bridges with unknown foundations. It is evident that an unknown percentage of the bridges identified by NBI with missing foundation data could also be highly vulnerable to scouring induced by water flow coupled with erodible soils. Thus, it is crucial to evaluate the bridge foundation characteristics, especially the type and depth of foundations, to determine the susceptibility to scour. Such evaluations are not viable for unknown bridge foundations since no design plans or as-built plans exist to reveal foundation type, depth, or geometry [2]. Non-destructive test (NDT) techniques have been identified as proper methods to gather unknown bridge foundations.

Various NDT methods have been developed and used in the past decades to assess the condition of civil infrastructure [3–6]. Among NDT methods, Sonic Echo /Impulse Response (SE/IR) is an economical method with a wide range of applications including characterizing unknown bridge

foundations. This method was initially used to evaluate the condition of bored cast-in-situ and pre-cast driven piles [7,8]. The method was then modified to evaluate the characteristics of unknown bridge foundations supporting bridge decks [9–12].

SE Test is conducted using the principle of longitudinal wave propagation in a long rod.

Consider the free vibration of an infinitely long rod with the cross-sectional area, A , Young’s modulus E , Poisson’s ratio ν , and density ρ , as shown in Figure 1 [13]. As the stress wave propagates along the rod and passes through the small element shown in Fig.1, axial stresses are generated on the left and right sides of the element. The dynamic equilibrium of the element requires that

$$\left(\sigma_{x_0} + \frac{\partial \sigma_x}{\partial x} dx \right) A - \sigma_{x_0} A = \rho A dx \frac{\partial^2 u}{\partial t^2} \quad (1)$$

Simplifying this equation will yield the one-dimensional equation of motion

$$\frac{\partial \sigma_x}{\partial x} = \rho \frac{\partial^2 u}{\partial t^2} \quad (2)$$

*Corresponding Author: email: srashidyan@yahoo.com



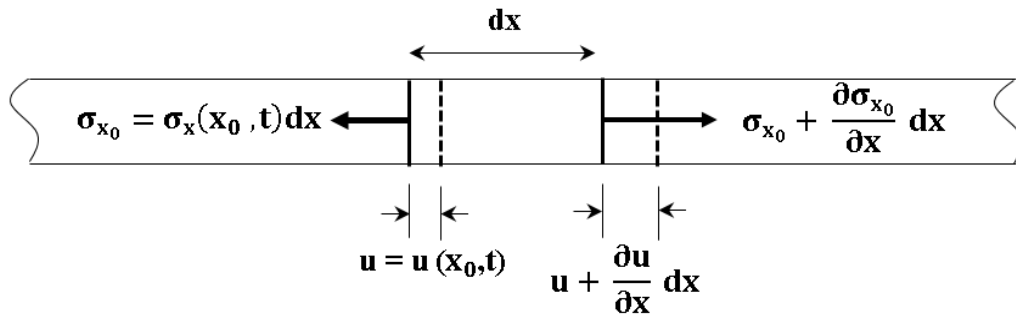


Fig. 1. Stresses and displacements at ends of the element of length dx and cross-sectional area, A [13].

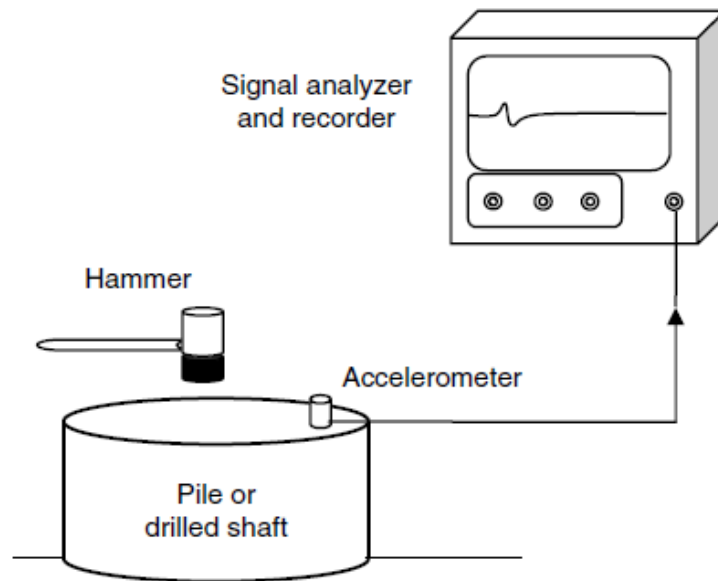


Fig. 2. Schematic of the SE test set-up [14].

For linear elastic materials, $\sigma_x = E\epsilon_x$, the equation becomes:

$$\frac{\partial^2 u}{\partial t^2} = v^2 \frac{\partial^2 u}{\partial x^2} \quad (3)$$

where v is the wave propagation velocity; for this case the wave travels at $v = \sqrt{E/\rho}$

Sonic Echo (SE) method, the longitudinal waves are generated by striking the top of the pile using a hammer as indicated in the SE/IR test setup depicted in Fig.2 [14]. Upon striking, a longitudinal wave with velocity v is generated along the pile. The generated wave travels down with velocity v and reaches the bottom of the pile. At this time, due to the change in impedance ($Z = EA/v$) of the materials, a part of

the wave energy will be transmitted through the interface to continue traveling in the soil (transmitted wave) and the remainder will be reflected at the interface toward the top of the pile as indicated in Fig.3. The impedance changes can be as a result of the change in pile section, concrete density, or pile-soil properties.

The reflected and transmitted waves are correlated to the incident wave at pile toe:

$$F_t = F_i \left(\frac{2Z_s}{Z_s + Z_p} \right) \quad (4a)$$

$$F_r = F_i \left(\frac{Z_s - Z_p}{Z_s + Z_p} \right) \quad (4b)$$

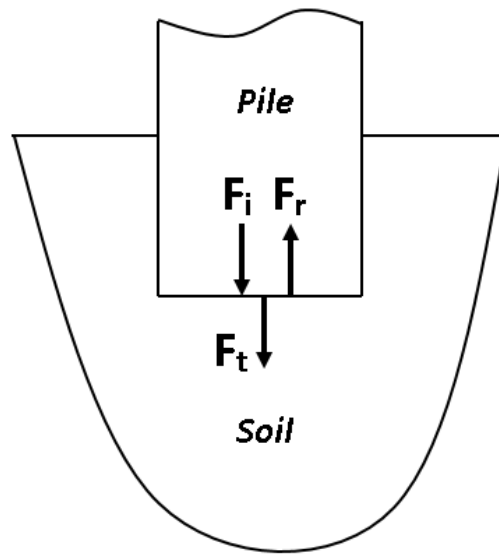


Fig. 3. Incident (F_i), reflected (F_r), and transmitted (F_t) waves at the pile-soil interface.

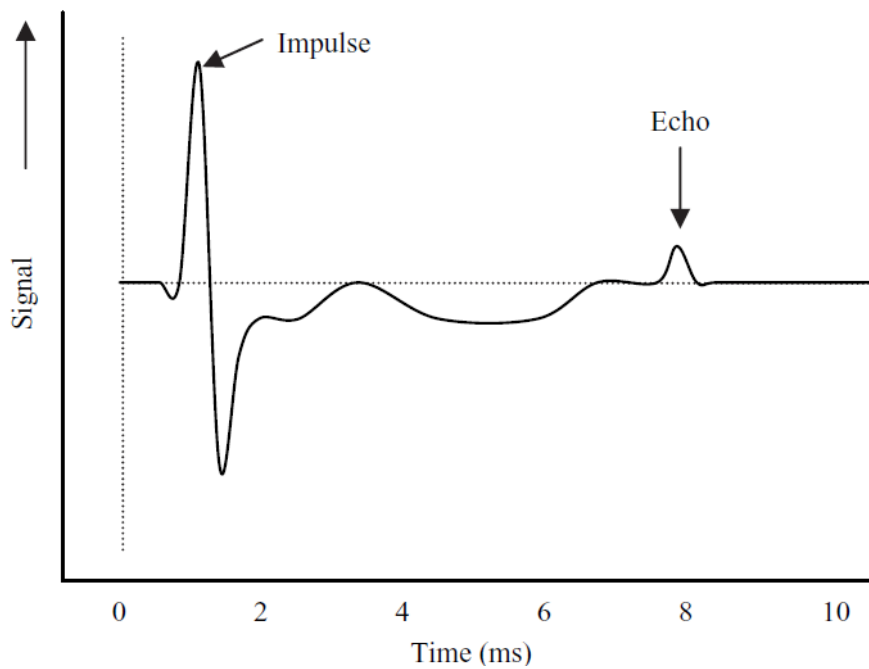


Fig. 4. A typical example of a Sonic-Echo velocity-time response plot [14].

Using a sensor (accelerometer or geophone velocity transducer) coupled to the pile head (see Fig.2), the time-lapse, t , between the hammer impulse and the arrival of the reflected waves at the pile head from the pile tip is then measured. A typical example of a Sonic Echo velocity (signal)–time response plot is indicated in Fig.4 [14].

The distance traveled by the stress wave will be the

product of time-lapse t between the impulse and echo and propagated wave velocity v . This distance is twice the pile length when the sensor is placed at the top of the pile. Finally, the length of the pile, L , can be calculated:

$$L = \frac{v \times t}{2} \tag{7}$$

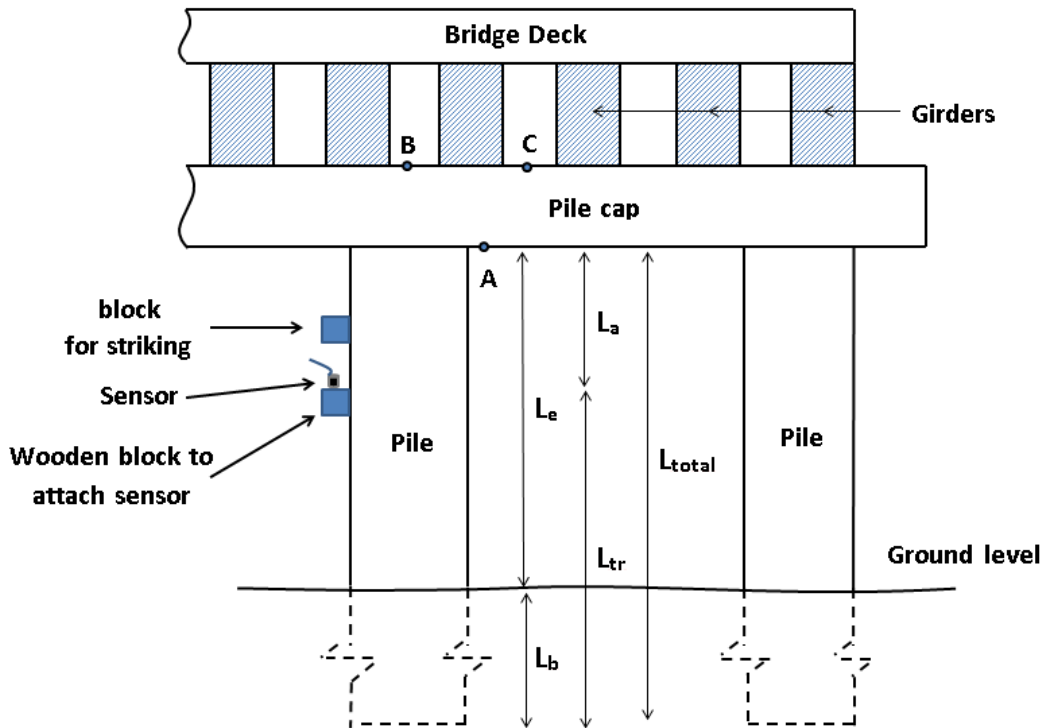


Fig. 5. Sonic Echo test setup for piles underneath bridges.

SE test setup indicated in Fig.2 can be modified to a proper setup to assess the conditions of the piles underneath a bridge deck. The modified setup is indicated in Fig.5. In this figure, the longitudinal waves can be generated by striking point B. Striking on a block attached to the side of the pile can also be used as another option. In the modified setup, the accelerometer can be placed vertically on a small block attached to the side of the pile. Given the propagated wave velocity, the total and buried length of the pile can be calculated using Eq. (6).

L_{tr} : Distance between sensor location and pile toe ($= (v \times \Delta t) / 2$)

(6.a)

L_{total} : Total length of pile = $L_{tr} + L_a$

(6.b)

L_b : Buried length of pile = $L_{total} - L_e$

(6.c)

Δt : Time difference between the impulse and first toe echo

v : Propagated wave velocity

The signals obtained from sensors can also be further investigated by Impulse Response (IR) analysis to support measurements obtained from SE tests. The force and velocity-time history signals are converted into the frequency domain using the Fast Fourier Transform. Mobility is then defined as the ratio between the converted frequency-base velocity and the frequency-based force. The result is commonly presented

as a plot of mobility versus frequency as shown in Fig.6. For the generated wavelengths greater than the diameter of a prismatic pile, there are resonant frequencies that depend on the pile length and the propagated wave velocity as shown in Figure 5 [14]. The length of the pile can be estimated from the difference of successive resonant frequencies (Δf) as:

$$L = \frac{v}{2 \times \Delta f} \quad (7)$$

Previous studies have shown that factors such as the pile-to-soil stiffness ratio, length-to-diameter ratio of the pile, presence of defects and anomalies near the pile head, striking method, and utilizing proper hammer are major factors affecting the success of the SE/IR test [15]. Ni et al. [10] showed that since the impact force energy is radiated from the piles into the surrounding soil, it is difficult to determine the length of a long pile with a high slenderness ratio. The maximum detectable pile length-to-diameter ratio reported in the literature varies from 10 to 30, depending on the stiffness ratio of the pile and the surrounding soil. It was also found that the SE method can be applied on drilled shafts if the shaft to soil stiffness ratio is more than 77 [16]. In addition, the determination of the length of a pile is affected by the presence of anomalies such as bulges and necks along the pile. A study showed that the defects with sizes greater than 10–

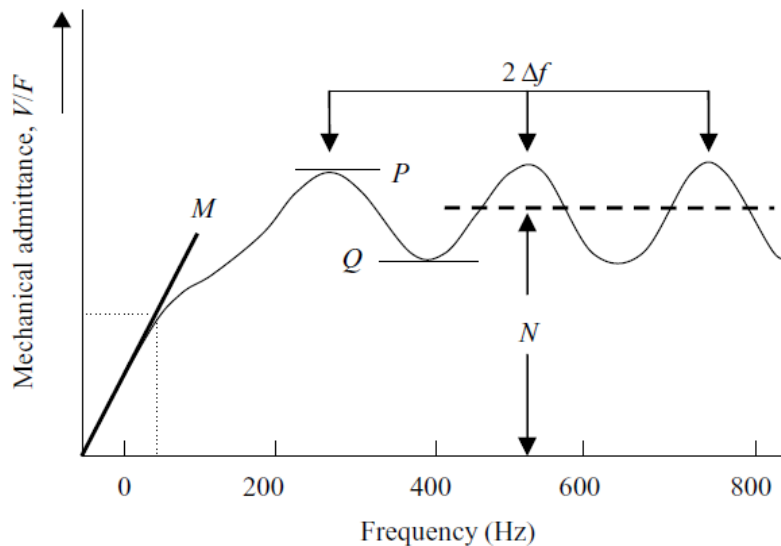


Fig. 6. Consecutive Resonant Frequencies on a Typical Mobility Graph [14]

30% can be identifiable by the SE method [17]. The striking method and hammer tip type can also affect the success of SE tests. Yin and Liu [15] have shown incorrect hammering can generate poor longitudinal waves. They also indicated that too small hammers with a stiff head generate high-frequency waves which attenuate fast and cannot reach the deeper part of the pile. In contrast, a too-large hammer with a soft head generates a wave with a large content of low frequencies and a large pile which may mix up with reflections from small defects in the shallow depth of the pile. Pandey and Anthony [18] conducted SE tests on 33 piles in four states. They investigated signals obtained from striking the bridge deck as well as an inclined lag screw inserted at 45 degrees to the side of the piles. They showed that using the lag screw had a better performance compared to striking on the top of the bridge deck. They have also showed that a sledgehammer with a medium density plastic tip provided reasonable results.

In another study, the effect of the striking method and hammer type on bridge foundations composed of reinforced concrete pier walls was investigated [19]. They compared the field test results with numerical analysis results and provided instructions to use proper hammer tips and striking methods. In addition to the abovementioned affecting factors, the accelerometer setup method can affect the quality of the obtained signals. Poor attachment methods result in unrepeatability signals which may result in inconsistent results. Anthony and Pandey [18] examined two attachment devices including a steel pin and a sheet metal screw attached to a metal block. Initial studies showed that the steel pin tended to loosen over time, causing poor transfer of stress wave information. They selected the sheet metal screw attached to an aluminum block as the superior sensor attachment method in their study. They also used two sensors aligned with each other along the axis of the pile and a fixed distance apart below the impact point. However, the results obtained from the two accelerometers were not compared together to provide

information regarding the effect of the sensor location on the quality of the signals.

Although previous studies have discussed various aspects of the affecting factors, there is a lack of useful investigation regarding the effect of the location of the sensor on the quality of the obtained signals. In the current study, the effect of sensor location on the success of SE tests conducted on woodpiles has been scrutinized by investigating the field results obtained from various sensor locations. Numerical simulations were also used to compare the theoretical and field test results and recommendations for better conducting the SE tests on unknown wood bridge foundations have been presented. The IR analysis was also conducted on the obtained velocity signals to provide more useful information. The results of this study can help engineers to place the sensors more effectively to obtain more successful SE tests.

2- Methodology

SE tests were performed on eight timber piles of three highway bridge foundations in New Mexico, USA. The number of the investigated piles and riverbed conditions are indicated in Table 1.

In this study, two accelerometers were attached to each pile and the length of the investigated piles was determined using the velocity and mobility graphs obtained from accelerometers. The wave speed for each pile was determined based on the time lapse between the two accelerometers. The measured pile lengths were compared to the actual lengths in Bridge 3 for which the foundation information was available to validate the results. Each test was repeated at least twice to ensure consistency. Numerical simulations of stress wave reflection were also performed to provide a better understanding of the effect of sensor location on the success rate of SE tests. IR analysis was also conducted on the data obtained from each accelerometer to provide more consistent results.

Table 1. Specifications of investigated bridge Foundations.

Bridge No.	Number of Tested Piles	Riverbed Condition
1	3	Dry
2	2	Running Water
3	3	Dry



Fig. 7. Accelerometers Mounted on a Pile Side Using Wooden Blocks.

The SE test procedure is presented here before discussing the results. The SE test procedure includes the selection of the method of striking, determining the accelerometer’s locations, equipment assemblage, and data acquisition.

Striking Setup

In the SE test, sonic waves are generated along the piles by striking the foundation. Depending on the accessibility of the pile top, different striking methods can be used to generate sonic waves along the pile. In piles, for which, either the entire or a portion of the pile top was accessible, vertical strikes on the top surface of the pile were applied. In contrast, for piles with inaccessible top, other options such as vertically striking the pile cap either downward on the top surface at Points B and C (See Fig.5) or a block attached to the side of the pile were used.

Receivers Setup

The sensor (accelerometer) is mainly placed atop the accessible pile top (such as wing piles). For piles with inaccessible top, the accelerometers were mounted on blocks attached to the side of the test pile with superglue. Examples of accelerometer attachment to the pile surface are indicated in Fig.7. Details of efficient sensor locations will be discussed later.

Hardware Assembly and Acquire Data

The utilized equipment was according to ASTM D5882-07-2013 [20] and ACI 228.2R-13 [21]. It consisted of a Freedom Data PC platform, two 100mv/g accelerometers, a 3-lb instrumented hammer with a force transducer, and various hammer tips. The hammer tips were hard, medium-hard, medium-soft, and soft with contact durations of 1200, 2400, 3600, and 4800 μs. The contact time increased with the degree of softness of the hammer tip.

3- Results and Discussion

3.1. Field tests results

To study the effect of accelerometer location, two accelerometers with different distances from the top of the piles were mounted on the side of the piles. The success rate of the performed SE tests is indicated in Table 2. In this table, D_1 and D_2 are the distances between the pile top and the location of the accelerometers 1 and 2 respectively. The location of accelerometer 1 from the pile top was selected between 0.3 to 0.76 m whereas they were 1 to 1.80 m for accelerometer 2.

The results indicated in Table 2 shows that some tests are not successful. This means the obtained signals are not interpretable and cannot be used to determine the depth of

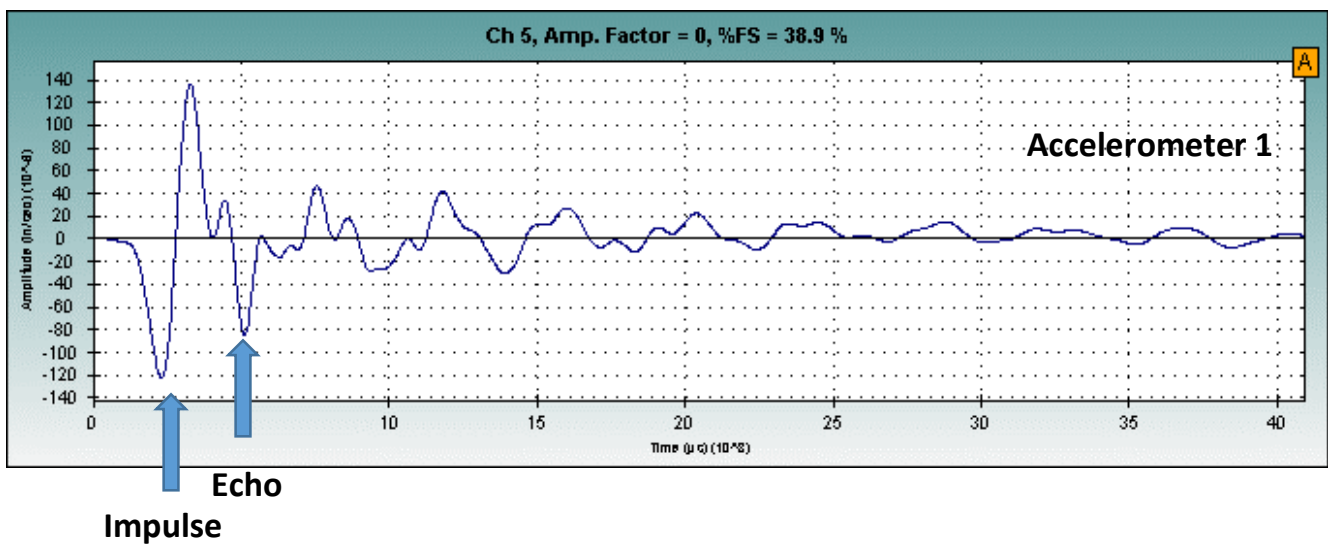
Table 2. The success rate of SE tests for accelerometers 1 and 2.

Bridge	Pile No.	D ₁ (m)	D ₂ (m)	Number of Tests	Number of Successful tests	
					Accelerometer 1	Accelerometer 2
1	1	0.6	1.07	6	4	3
	2	0.53	1	4	2	0
	3	0.71	1.17	3	3	2
2	1	0.76	1.80	21	16	14
	2	0.3	1.37	24	24	24
3	1	0.3	1.22	12	8	3
	2	0.3	1.52	12	11	9
	3	0.3	1.52	12	11	10
Sum				94	79	66
Success Rate (%)					84	69.1

the piles. Factors such as attenuation of the wave energy, improper hammering, background noise, and so on can result in unsuccessful tests. The data provided in Table 2 also show that if the accelerometers are located 0.3 to 1.8 m from the top of the pile, success rates between 69.1 to 84 percent can be achieved. However, the inferred lengths of the piles were more consistent from the top accelerometer than the accelerometer mounted closer to the ground level. The success rate of the SE tests from accelerometer 1 was 21.6% greater than accelerometer 2. The velocity signals obtained from the accelerometer closer to the top of the pile showed less complication than the farther accelerometer. More explanation on this is presented in the sequel.

To discuss good versus bad results, two velocity signals obtained from the top and bottom accelerometers mounted

on one of the investigated piles are indicated in Fig.8. Good signals were considered as signals for which both impulse and echo are distinguishable whereas bad signals were those which did not have either clear impulse or echo. Fig.8a shows that both impulse and echo are distinguishable. The pile toe echo amplitude is significantly greater than the next valleys on the waveform. In contrast, the echo is not obvious on the signal obtained from the bottom accelerometer (2) in Fig.8b. Two consecutive valleys with similar amplitudes (indicated with black arrows in Fig.8b) exist after the impulse, therefore it is not clear that which of these valleys corresponds to the pile toe echo. Consequently, determining the length of the pile using the signal obtained from the bottom accelerometer is not possible in this figure.



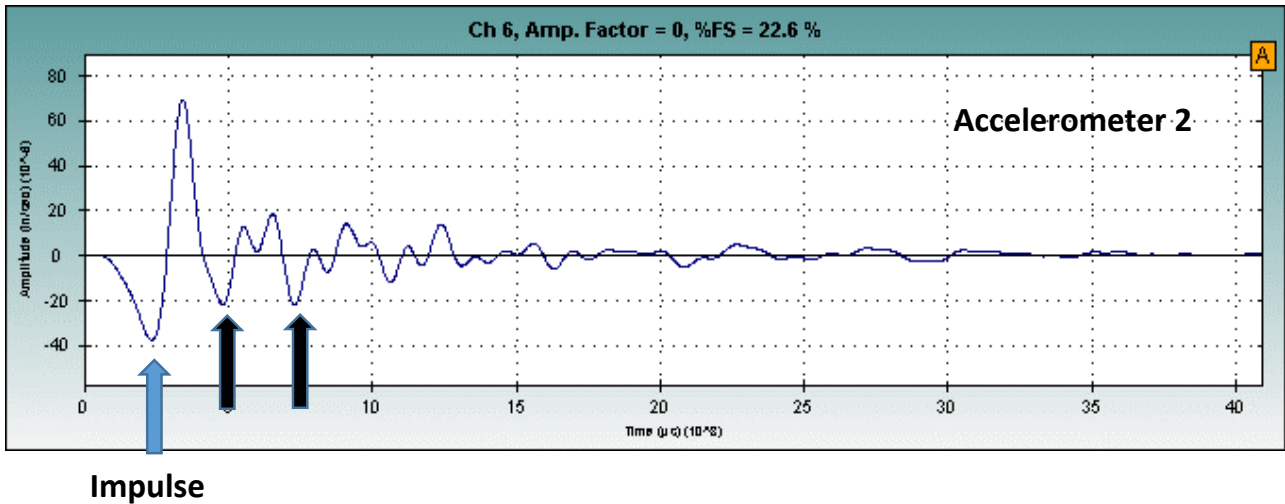


Fig. 8. Two velocity signal examples obtained from the top (a) and bottom accelerometers (b) mounted on the investigated piles.

To reveal more information on the effect of the accelerometer’s distance from the pile top, it was decided to mount accelerometer 2 (bottom accelerometer) significantly farther from the pile top in one of the SE tests conducted on pile 1 in Bridge 1. This allowed not only to better study the signal obtained from an accelerometer mounted further but also to calculate the velocity of the propagated wave. The calculations are described as follows.

Two accelerometers were placed far apart ($D_1=0.45$, $D_2=2.45$ m) so that the arrival times at the two sensors were distinguishable. Accelerometer 1 was closer to the top of the pile while accelerometer 2 was adjacent to the ground surface. The time difference between the two arrival times of the wave at each accelerometer was used to determine the wave velocity. The velocity graphs of accelerometers 1 and 2 are shown in Fig.9.

Points A and B show the first arrival times at accelerometers 1 and 2 respectively. The time-lapse (Δt) between points A and B was used to estimate the wave velocity. Since the distance between accelerometers (ΔL) is 2m and $\Delta t = 1.96 - 1.46 = 0.5$ ms, the wave velocity is estimated as:

$$v = \frac{\Delta L}{\Delta t} = \frac{2}{0.0005} = 4000 \text{ m/s} \quad (8)$$

The measured wave velocity is within the expected range of wave velocity for wood [22].

The signals indicated in Fig.9 also show that the shape of these two velocity graphs is different for the two sensors. For accelerometer 1, both impulse and echo are clear and their corresponding Δt was found 2.76 ms and the calculated length of the pile is 6 m using 4000 m/s as the propagated wave velocity.

For accelerometer 2, many echoes exist on the velocity graph. Point C shows the location of the impulse; however, the location of the pile toe echo is not clear. The time difference between Points C (first valley) and D (second valley) is 1.62 ms. The estimated distance between the sensor and the bottom is:

$$L_{tr} = \frac{v \times \Delta t}{2} = \frac{4000 \times 1.62 \times 10^{-3}}{2} = 3.24 \text{ m} \quad (9)$$

Since the distance between the accelerometer and pile top is 2.46, the total pile length is estimated as $L_{total} = 3.24 + 2.46 = 5.7$ m. This value is close to the estimated pile length from accelerometer 1 (6 m). The reflected wave continued to go upward, is then reflected at the pile top, and became a down-going wave arriving at the sensor at Point E. Since the distance between the accelerometer and pile top is 2.46 m, the wave travels 4.92 m (ΔL) before returning to the accelerometer. The required time for this path is:

$$\Delta t = \frac{\Delta L}{v} = \frac{4.92}{4000} = 0.00123 \text{ sec} = 1.23 \text{ ms} \quad (10)$$

This calculated time is close to the time difference between Points D and E in Figure 9b.

The above-mentioned calculations show that the multiple peaks observed at the accelerometer located far from the pile top were related to the multiple reflections from both the top and the bottom of the pile. The accelerometer closer to the top of the pile provides results that were easy to interpret. Reflections from both ends can complicate the velocity

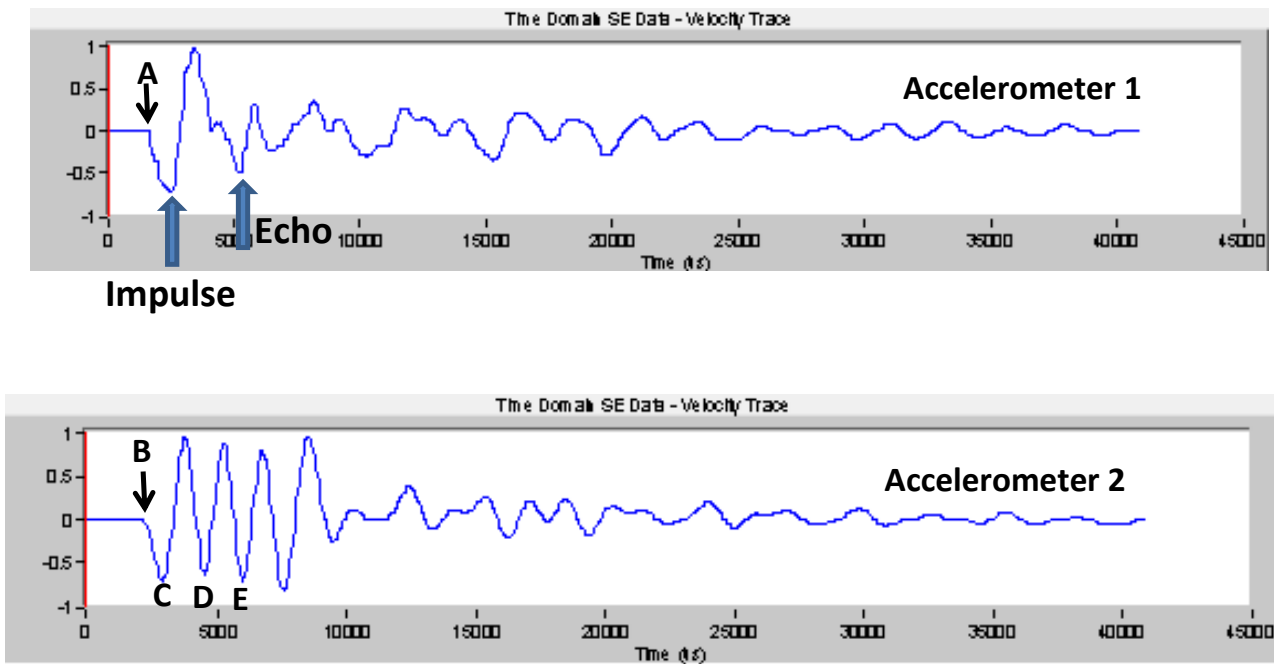


Fig. 9. Velocity Graphs of Accelerometers 1 and 2 in a Test pile of Bridge 1.

V (wave velocity)	4000 m/s
E (modulus of elasticity)	10.28 GPa
ρ (density)	800 kg/m ³
ν (Poisson's ratio)	0.3
Impulse shape	Parabola
Impulse duration	1.2 ms
Simulation time duration	20 ms
Elements type	C3D8R (8-node linear brick)

Table 3. Specifications of Finite Element Model of the Selected Pile.

graphs as indicated in Fig.9b for accelerometer 2. The complementary discussion will be presented later in the finite element analysis section.

It should be noted that other factors such as reflections from the superstructure, ambient noise existing in the ground, and layered soils may also affect the results which have not been discussed here. Only a comparison between success rates obtained from different accelerometers has been made based on the clarity of the pile toe echoes on the signals.

3.2. Numerical simulation results

To study the nature of the velocity signals obtained from the sensors with different distances from the pile top, it was decided to simulate the test pile investigated in the previous section. The selected FEM model has the same dimension

as the tested pile. Although the selected numerical model consists of an individual pile with no superstructure, it can provide valuable information regarding the effect of the sensor location on the SE test results. The length of the tested pile ($L = 6$ m) was calculated based on the field test results in the previous section. The simulated FEM model provides means to compare signals obtained from different nodes on the side of the pile with each other. Other properties of the model are indicated in Table 3. These properties are in accordance with the Wood Handbook (United States Department of Agriculture Forest Service, 2010). The assumed wave velocity is 4000 m/s which is the same as the velocity calculated in the previous section. In the wave propagation problems, the element size should be less than about 1/8–1/10 of the wavelength of the highest frequency to capture the proper response [23]. The

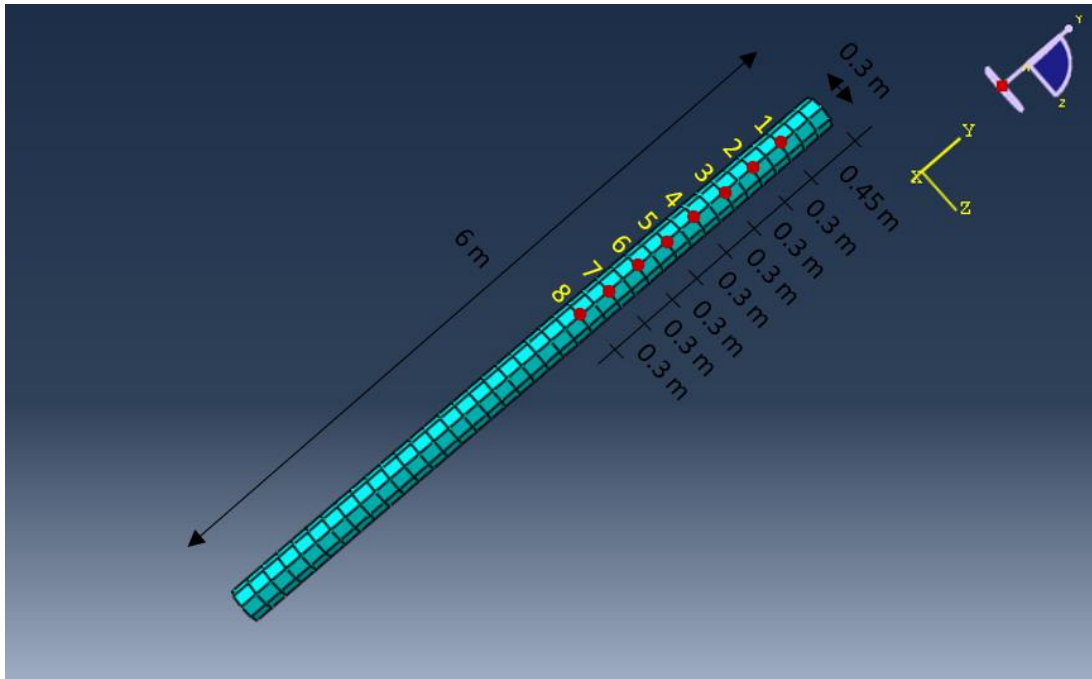


Fig. 10. Simulated FEM pile model to investigate the Effect of Sensor Location on SE test results.

maximum frequency of the propagated stress wave is about $2.5/\tau$ [24]; where τ is the duration of impact. Since the wave velocity is 4000 m/s, throughout this study, the maximum sizes of the finite elements were selected as 0.15 m which satisfies the above-mentioned limitation.

Fig.10 shows the simulated FEM model. Since a part of the pile top was accessible in the field, vertical striking had been applied at the top surface of the pile. Therefore, downward strikes at the pile top surface were applied as the source in the FEM model. Since the velocity graphs lose some of their frequency contents during integration, it was decided to investigate acceleration graphs at nodes to provide more details on the nature of propagation. The acceleration graphs obtained from nodes 1, 3, 6, and 8 are indicated in Fig.11 as examples. It should be noted that Nodes 1 and 8 approximately correspond to the locations of the accelerometer 1 and 2 in the field which were discussed in the previous section ($D_1=0.45$, $D_2=2.45$ m).

Fig.11a shows that when the node is located at 0.45m from the pile top, the obtained acceleration graph is interpretable. The impulse and echoes were completely detectable on the acceleration graph. The blue arrow shows the location of the impulse whereas the orange arrows show the location of the echoes from pile toe. The length corresponding to the time differences between the impulse and echo is very close to the actual length (The error is less than %5) based on the following calculations:

$$L_{tr} = \frac{v \times \Delta t}{2} = \frac{4000 \times (0.0032 - 0.0003)}{2} = 5.80 \text{ m} \quad (11)$$

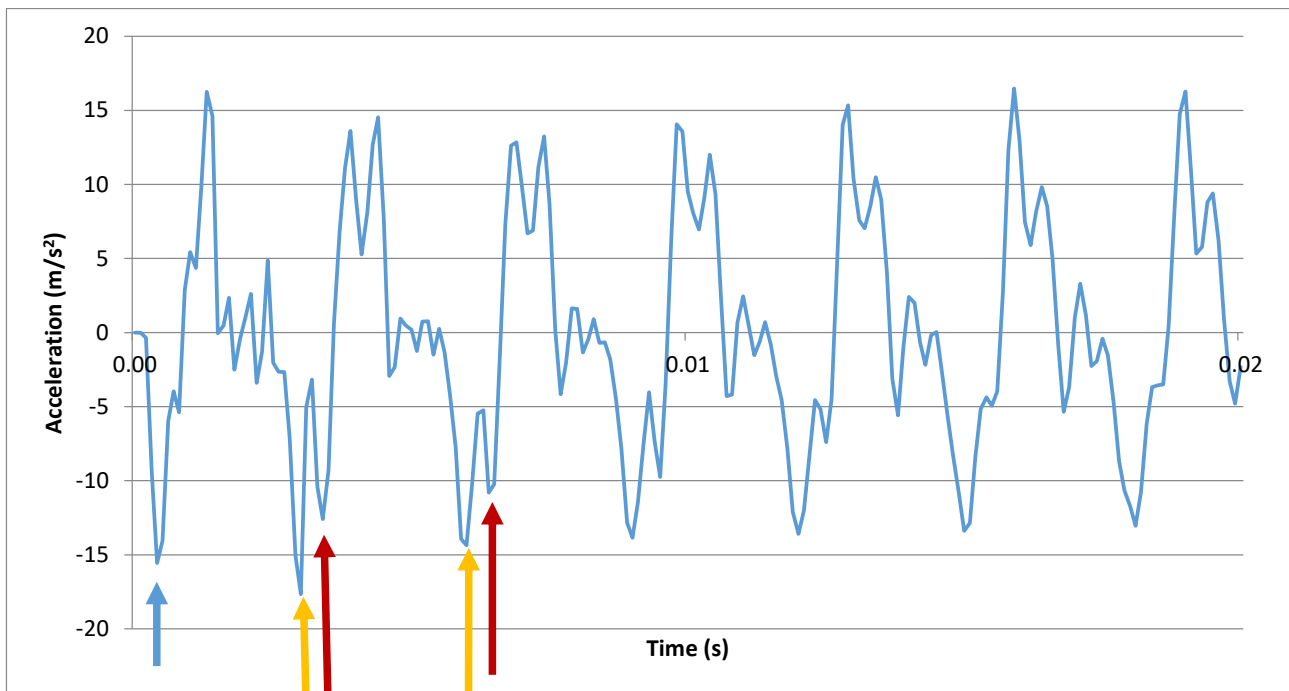
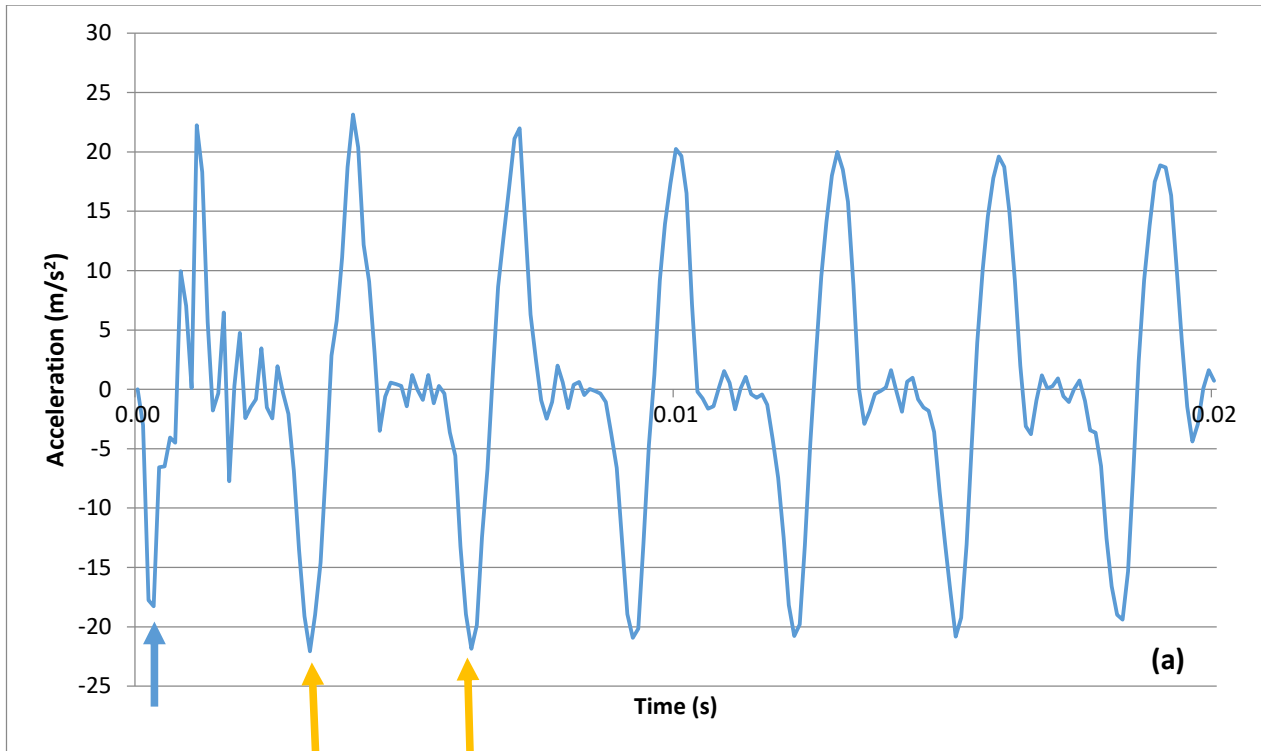
$$L_{total} = L_{tr} + L_a = 5.80 + 0.45 = 6.25 \quad (12)$$

$$\text{ERROR} = \frac{(6.25 - 6)}{6} \times 100 = 4.16\% \quad (13)$$

On the other hand, for nodes located farther from the pile top, the reflected wave from the pile toe and pile top make two closely spaced consecutive valleys on the waveform. In Fig.11b, f and h two sets of valleys indicated with orange and red arrows imply the reflections from the pile toe and pile top respectively. The waveform shape becomes more complicated when the node is located farther from the pile top. The waveform becomes even more complicated when the node is located 2.4 m below the pile top (very close to the middle of the pile). The waveform indicated in Fig.11d contains large-amplitude reflections from the pile top which might be mixed up with the pile toe reflection. Therefore, when the accelerometer is mounted too far from the pile top, the echo from the pile toe may not be distinguishable due to the presence of multiple similar valleys on the waveform.

3.3. IR Analysis Results

The IR analysis (based on the frequency content of the entire waveform) was carried out on six piles of Bridges 1 and 3 to support the SE test results. The length of the piles was determined by measuring the differences between the consecutive resonant frequencies (see Fig.6) and substituting in Eq. (7). The success rate of IR analysis in determining the length of the piles is summarized in Table 4. The results indicated in Table 4 show that the inferred length



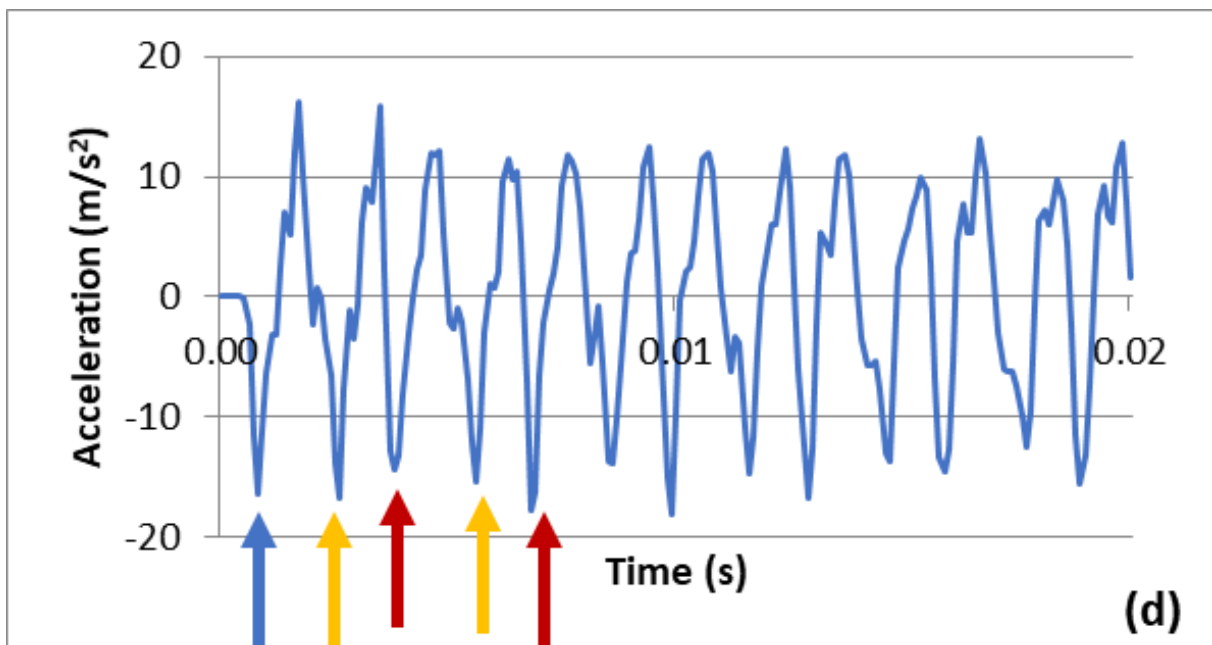
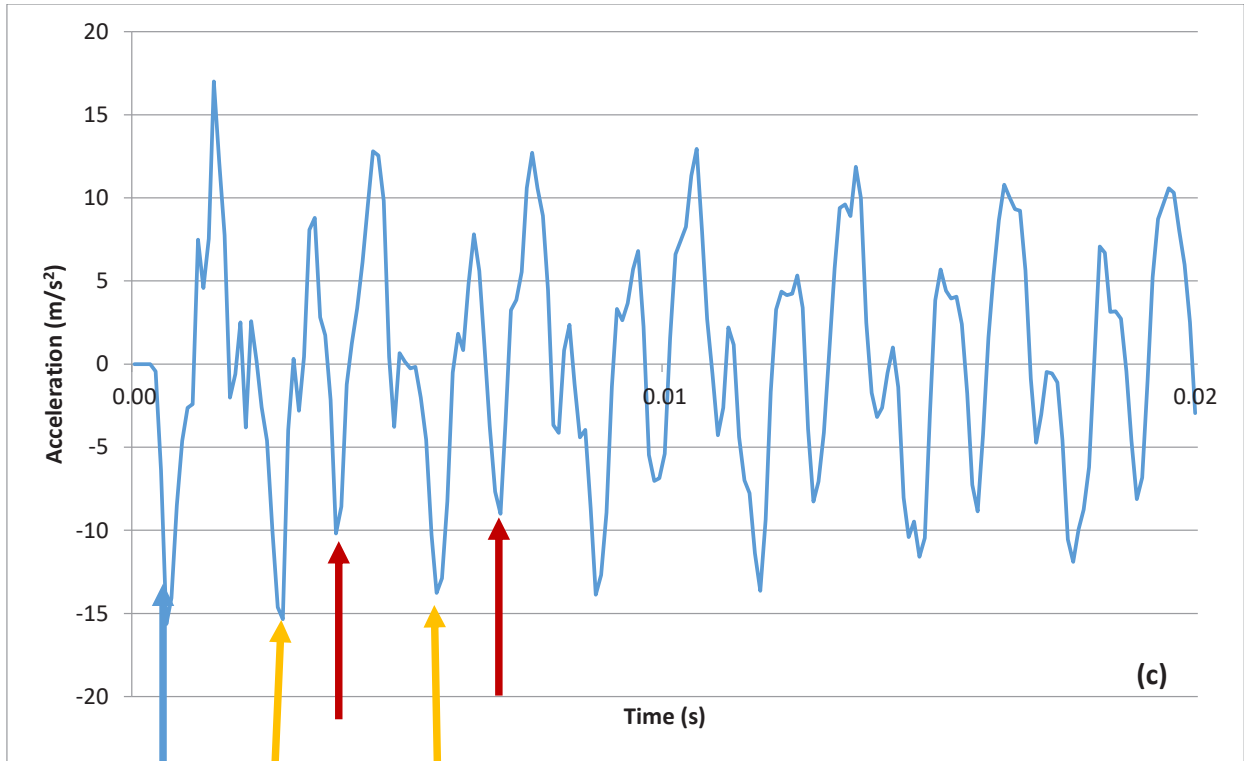


Fig. 11. Acceleration Amplitude-time graphs obtained from nodes 1, 3, 6, 8 (from a to d, respectively).

Table 4. The success rate of IR analysis based on Accelerometer 1 and 2 data.

Bridge	Pile Name	Number of Tests	Number of Successful tests	
			Accelerometer 1	Accelerometer 2
1	1	6	5	4
	2	4	0	0
	3	3	0	3
3	1	12	11	6
	2	12	2	2
	3	12	10	11
	Sum	49	28	26
	Success Rate (%)		57.1	53.1

of the pile was somewhat more consistent from the top accelerometer than the accelerometer mounted closer to the ground level. The success rate for accelerometer 1 is 7.7% greater than accelerometer 2. The results also show that the success rate of IR analysis is generally less than SE tests (see Table 2). This observation is in accordance with previous studies on woodpiles [18] Therefore, SE tests seem to produce more success compared to IR analysis based on our data available for the investigated bridge foundations.

4- Conclusions

SE/IR method is a versatile NDT method to characterize unknown bridge foundations. Although the method is easy to conduct many factors such as the hammering quality, reflections from the superstructure, surrounding soils, the striking method can affect the signals obtained from the sensors. In the current study, the effect of sensor location on the success rate of SE tests is investigated. SE tests were carried out on 8 bridge piles with known and unknown depths to study the effect of sensors location, on the obtained signals. The results obtained from two accelerometers mounted on the investigated piles show that when the distances between the accelerometer and the pile top were within 0.30 to 1.80 m, interpretable velocity graphs were achieved. However, the measured length of the pile was more consistent from the top accelerometer (which was mounted 0.3 to 0.75m below pile top) than the accelerometer mounted closer to the ground level. The success rate of the SE tests from the top accelerometer was 21.6% greater than the bottom accelerometer. The velocity signals obtained from the accelerometer closer to the top of the pile showed less complication than the accelerometer placed further. The observations also show that the accelerometer located too far from the pile top was affected more by reflections from both ends such that the pile toe echo was no longer detectable. This was confirmed by numerical simulations of a pile model with the same dimension as one of the investigated piles. The waveform obtained from nodes further from the top of the pile contained large-amplitude reflections from the pile toe

which could mislead identification of the pile toe reflection. Also, the conducted IR analysis showed that the inferred length of the piles was somewhat more consistent from the top accelerometer than the accelerometer mounted closer to the ground level. The success rate for the top accelerometer was 7.7% greater than the bottom accelerometer. The results also show that the success rate of IR analysis is generally less than SE tests. As a result, to attain more success in determining the pile length, it is recommended not to mount the accelerometer too far from the pile top. It is expected that the distances between 0.3 to 0.7 m from pile top create satisfactory results.

Acknowledgment

This study is partially supported by the New Mexico Department of Transportation. The authors would like to thank Ms. Michelle Mann (New Mexico Department of Transportation) and Dr. Thiet Nguen (Federal Highway Administration) for their valuable suggestions and Mr. Ali Jwary for his assistance during performing the tests.

Notation

A	Cross sectional area
V	Wave velocity
E	Young's modulus
ν	Poisson's ratio
ρ	Density
Z	Impedance
L_{tr}	L Distance between sensor location and pile toe
L_{total}	Total length of the pile
L_b	Buried length of the pile
Δt	Time difference between the impulse and first toe echo

References

- [1] M.A. Mulla, Evaluating Bridges with Unknown Foundations for Vulnerability to Scour, (2014) 3.
- [2] J.T. Coe, J.E. Nyquist, B. Kermani, L. Sybrandy, Application of non-destructive testing to evaluate unknown foundations for Pennsylvania bridges, Pennsylvania. Dept. of Transportation. Bureau of Planning and Research, 2013.
- [3] J.M. Amir, E.I. Amir, Testing of bored pile inclination, in: Proceedings of the 9th International Conference on Testing and Design Methods for Deep Foundations (IS-Kanazawa 2012), 2012.
- [4] N. Chidambarathanu, Processing Digital Image for Measurement of Crack Dimensions in Concrete, Civil Engineering Infrastructures Journal. (2019).
- [5] Rashidyan, Maji Arup, Ng Tang-tat, Performance of Nondestructive Parallel Seismic Testing Method in Determining Depth of Shallow Foundations, Journal of Performance of Constructed Facilities. 33 (2019) 06019001. Doi: 10.1061/(ASCE)CF.1943-5509.0001288.
- [6] S. Rashidyan, T. Ng, A. Maji, Practical Aspects of Nondestructive Induction Field Testing in Determining the Depth of Steel and Reinforced Concrete Foundations, J Nondestruct Eval. 38 (2019) 19. doi:10.1007/s10921-019-0557-x.
- [7] F. Rausche, G.G. Goble, Determination of pile damage by top measurements, in: Behavior of Deep Foundations, ASTM International, 1979.
- [8] A.J. Weltman, Integrity testing of piles: a review, Construction Industry Research and Information Association, 1977.
- [9] R.J. Finno, S.L. Gassman, P.W. Osborn, Non-destructive evaluation of a deep foundation test section at the Northwestern University national geotechnical experimentation site, A Report Submitted to the Federal Highway Administration Office, Northwestern University, Evanston, Illinois. (1997).
- [10] S.-H. Ni, L. Lehmann, J.-J. Charng, K.-F. Lo, Low-strain integrity testing of drilled piles with high slenderness ratio, Computers and Geotechnics. 33 (2006) 283–293.
- [11] L. Olson, F. Jalinoos, M.F. Aouad, Determination of Unknown Subsurface Bridge Foundations: A Summary of the NCHRP 21-5 Interim Report, Geotechnical Engineering Notebook, Geotechnical Guideline. (1998).
- [12] S. Rashidyan, T. Ng, A. Maji, Bridge Foundation Depth Estimation Using Sonic Echo Test, in: C. Sciammarella, J. Considine, P. Gloeckner (Eds.), Experimental and Applied Mechanics, Volume 4, Springer International Publishing, 2016: pp. 99–106.
- [13] S. Kramer, Geotechnical Earthquake Engineering, Pearson, 1996.
- [14] B. Hertlein, A. Davis, Nondestructive Testing of Deep Foundations, John Wiley & Sons, 2007.
- [15] J. Yin, J. Yuan, M. Liu, Assessment of pile integrity by low-strain stress wave method, HKIE Transactions. 6 (1999) 42–49.
- [16] D.S. Kim, H.W. Kim, Effects of surrounding soil stiffness and shaft length in the impact-echo test of drilled shaft, KSCE Journal of Civil Engineering. 7 (2003) 755–762.
- [17] Y.-H. Huang, S.-H. Ni, K.-F. Lo, J.-J. Charng, Assessment of identifiable defect size in a drilled shaft using sonic echo method: Numerical simulation, Computers and Geotechnics. 37 (2010) 757–768.
- [18] R.W. Anthony, A.K. Pandey, Determining the Length of Timber Piles in Transportation Structures, (2005).
- [19] S. Rashidyan, T. Ng, A. Maji, Estimating the Depth of Concrete Pier Wall Bridge Foundations Using Nondestructive Sonic Echo, Journal of Nondestructive Evaluation. 36 (2017) 56.
- [20] American Society for Testing Materials, Standard Test Method for Low Strain Impact Integrity Testing of Deep Foundations, (2013).
- [21] American Concrete Institution, Report on Nondestructive Test Methods for Evaluation of Concrete in Structures, (2013).
- [22] United States Department of Agriculture Forest Service, Wood Handbook, Wood as an Engineering Material, (2010).
- [23] Y. Lin, M. Sansalone, N.J. Carino, Impact-echo response of concrete shafts, Geotechnical Testing Journal. 14 (1991) 121–137.
- [24] N.J. Carino, M. Sansalone, N.N. Hsu, Flaw detection in concrete by frequency spectrum analysis of impact-echo waveforms, International Advances in Nondestructive Testing. 12 (1986) 117–146.

HOW TO CITE THIS ARTICLE

S. Rashidyan, T.-T. Ng, A. Maji, Study of the Effect of Sensor Location on Sonic Echo/Impulse Response Testing in Timber Piles, AUT J. Civil Eng., 4(4) (2020) 473-486

DOI: [10.22060/ajce.2020.16552.5590](https://doi.org/10.22060/ajce.2020.16552.5590)

